Theories of Reaction Rates

Quantitative relationship between reaction rate constant and temperature given by Arrhenius Equation:

$$k = Ae^{-E_a/RT} \qquad (1)$$

where k is the rate constant, A is the **frequency factor**, and E_a is the **activation energy**.

Eq. (1) indicates that the rate constant of a reaction is essentially the product of an *"attempt rate"* or *collision frequency*, A, and the *fraction of molecules having an energy E_a or greater*, which is given by the Boltzmann factor, E_a/RT.

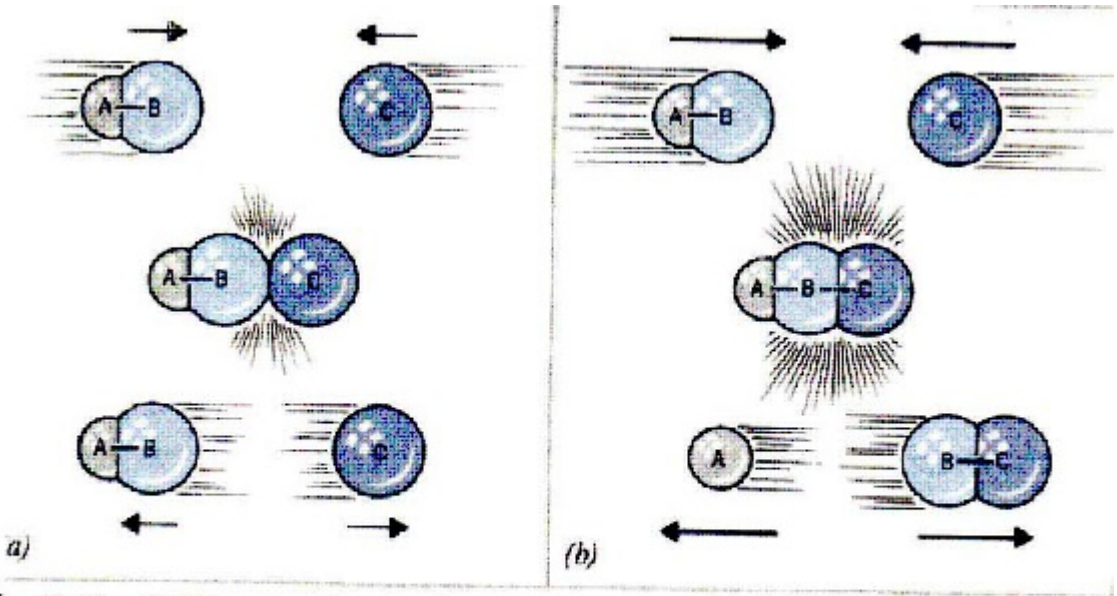

Fig. 19.10. *(a)* When two slow-moving molecules collide, their electron clouds cannot interpenetrate much and they just bounce off each other, chemically unchanged. *(b)* When fast-moving molecules collide, atoms approach each other much more closely as their electron clouds interpenetrate. This can lead to bond making and bond breaking. The net change here is $AB + C \rightarrow A + BC$.

This energy requirement for an "effective" collision can be viewed as a *potential energy barrier* that must be surmounted if a reaction is to occur, and can be represented by the familiar **energy profile** of the reaction:

Figure 15.8

Arrhenius plots in the form $\log_{10}k$ versus $1{,}000/T$ for three unimolecular and three bimolecular reactions. The Arrhenius equation (Equation 15.35) predicts that these plots should be linear with slopes $-E_a/[(1000)(2.303)R]$ and y-intercepts $\log_{10}A$. Experimental values of E_a and $\log_{10}A$ for these and other reactions can be found in Table 15.4. When measurements extend over larger temperature ranges, slight curvature is sometimes found, usually attributed to a slight temperature dependence of A (as predicted by reaction rate theory; see Section 15.4).

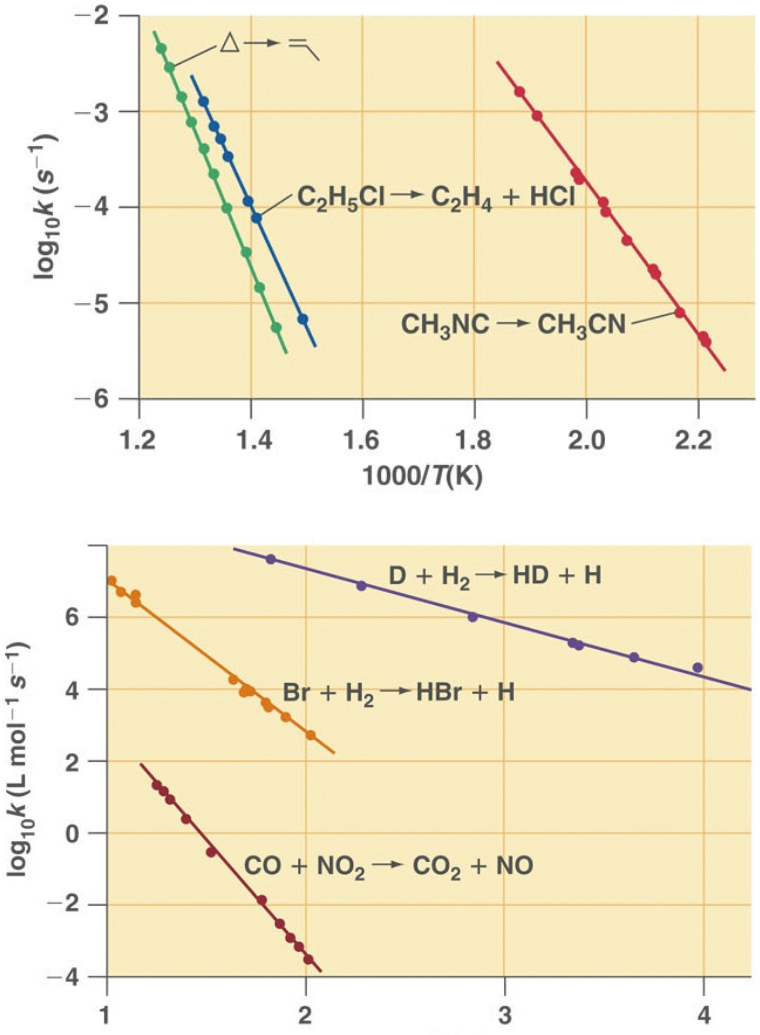

Figure 15.9

(a) Energy profile for a "typical" exothermic elementary reaction $A + B \longrightarrow P$. $AB^{\ddagger}$ is the "transition state" and E_a' is the activation energy for the reverse reaction. Also shown are Boltzmann energy distributions at two temperatures, illustrating the great increase in the fraction of molecules with $E > E_a$ as T rises. **(b)** Energy profiles for the reactions whose Arrhenius plots were shown in Figure 15.8.

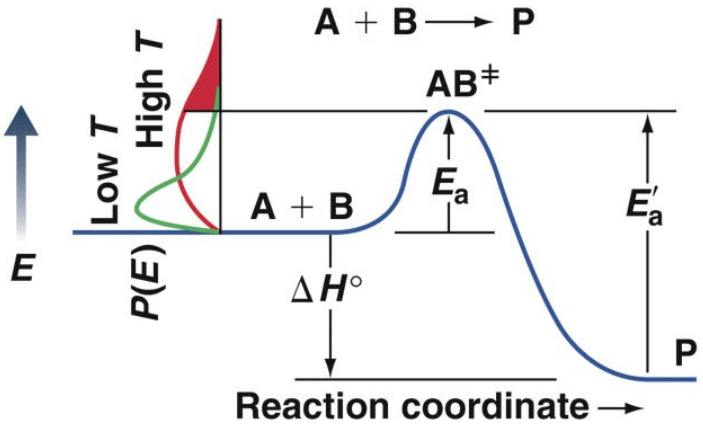

(a)

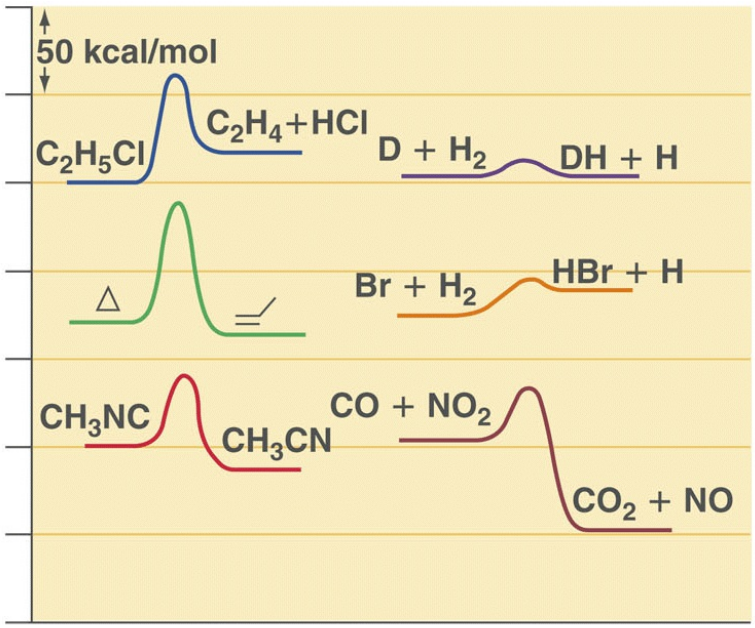

(b)

Assuming that the (usually small) difference between U and H can be ignored, $\Delta_r U^\circ \approx \Delta_r H^\circ$ for most reactions, and, hence, $E'_a = E_a - \Delta_r H^\circ$, where E'_a is the activation energy for the reverse reaction. Thus, because for an exothermic forward reaction, $\Delta_r H^\circ < 0$ and $E'_a > E_a$, the reverse reaction may be many orders of magnitude *slower* than the forward reaction. By contrast, for an endothermic reaction, $\Delta_r H^\circ > 0$ and $E'_a < E_a$, and the reverse reaction is *faster* than the forward one. If both k and k′ can be represented by the Arrhenius Equation, their ratio is given by

$$\frac{k}{k'} = \frac{Ae^{-E_a/RT}}{A'e^{-E'_a/RT}} = \frac{A}{A'}e^{-\Delta H_r^\circ/RT} \qquad (2)$$

which represents the same temperature dependence that is shown by the equilibrium constant in the van't Hoff Equation:

$$\frac{d\ln K}{d(1/T)} = -\frac{\Delta H^\circ}{R} \qquad (3)$$

as it must, according to the principle of detailed balance:

$$K = \frac{k}{k'} \qquad (4)$$

In addition, because

$$K = e^{-\frac{\Delta_r G^\circ}{RT}} = e^{-\left(\frac{\Delta_r H^\circ}{RT} - \frac{\Delta_r S^\circ}{R}\right)} \tag{5}$$

then

$$\frac{A}{A'} = e^{-\frac{\Delta_r S^\circ}{R}} \tag{6}$$

which implies that the ratio of "attempt rates" (A/A′) depends on the relative entropies of the reactants and products. Thus, if $\Delta_r S^\circ < 0$, for example, then the reactants attempt to react at a lower frequency than the products attempt to fall apart into reactants. Additionally, the frequency factors, A and A′, must have a slight temperature dependence, since $\Delta_r S^\circ$ does. Typically, however, the overriding temperature dependence is that in the exponential Boltzmann factor.

Molecular Theories of Elementary Reactions

Collision Theory

The so-called collision theory treats E_a as a potential energy barrier and then develops a molecular model for the frequency factor A. According to the kinetic theory of gases, the frequency of collisions between like molecules in a gas is given by

$$Z_{mol} = \sqrt{2}\frac{N}{V}\bar{v}\pi d^2 = \sqrt{2}\,[X]\bar{v}\pi d^2 \qquad (7)$$

where Z_{mol} is the average number of collisions made by one X molecule per unit time, $N/V = [X]$ is the number of X molecules per unit volume (*i.e.,* the concentration), and πd^2 is the mutual molecular area of collision for molecules having a diameter of d.

For the frequency of collisions between *dissimilar* reactant molecules A and B, the average velocity $\bar{v}$ must be replaced by the *average* <u>*relative*</u> *velocity* $\bar{v}_{rel}$ between A and B, given by

$$\bar{v}_{rel} = \sqrt{\frac{8k_B T}{\pi\mu}} \qquad (8)$$

where k_b is Boltzmann's constant, and μ is the *reduced mass* of A and B:

$$\mu = \frac{m_A m_B}{m_A + m_B} \qquad (9)$$

The total frequency of A-B collisions per unit volume is then

$$Z_{AB} = \bar{v}_{rel}\pi d_{AB}^2 [A][B] \qquad (10)$$

where d_{AB} is the mean A-B collision diameter, given by $d_{AB} = (d_A + d_B)/2$, with d_A and d_B being the molecular diameters of A and B. (The factor $\sqrt{2}$ in Eq. (7) is included to avoid counting collisions of A and B molecules twice because in A-A and B-B collisions the two colliding molecules are indistinguishable. But this factor is not included in Eq. (10) because in A-B collisions the two molecules are distinguishable.) The quantity πd_{AB}^2 is called the *collision cross section.*

Thus, the overall reaction rate is the frequency of potentially reactive collisions, Z_{AB}, multiplied by the fraction of colliding molecules that have sufficient energy to react, $e^{-E_a/RT}$, resulting in the following expression for the rate of an elementary bimolecular reaction:

$$Rate = \bar{v}_{rel}\pi d_{AB}^2 e^{-E_a/RT}[A][B] \qquad (11)$$

Therefore, because the rate of a bimolecular reaction is Rate = k[A][B], the bimolecular rate constant k and the frequency factor A can be identified in Eq. (11) as:

$$k = \bar{v}_{rel}\pi d_{AB}^2 e^{-E_a/RT} \qquad (12)$$

and

$$A = \bar{v}_{rel}\pi d_{AB}^2 = \sqrt{\frac{8k_B T}{\pi\mu}}\pi d_{AB}^2 \qquad (13)$$

Thus, A is predicted to increase with temperature as $T^{1/2}$, which is a relatively mild temperature dependence that is typically masked by the exponential term. In addition, k also should increase with decreasing μ, in agreement with Graham's Law of effusion.

In essence, the frequency factor A represents an upper limit to the magnitude of k, corresponding to $E_a = 0$, *i.e., every collision* results in reaction. Depending on the particular reaction system, this upper limit can vary over a sizable range, but is typically ~10^{-10} cm^3/molecule/s, or ~10^{11} L/mol/s.

The Table below compares experimentally observed A factors ($\log_{10}A$) with those predicted by collision theory ($\log_{10}A_{ct}$) from Eqs. (12) and (13) for a variety of elementary bimolecular reactions. Most of the experimentally measured A factors are considerably smaller than those predicted by collision theory, with the disagreement expressed as the ratio $p = A/A_{ct}$, where p is the so-called *steric factor*.

TABLE 15.4

Arrhenius parameters for selected bimolecular gas-phase reactions[a]

Reaction	E_a	$\log_{10}A$	$\log_{10}A_{ct}$	Steric factor p
$Na + Cl_2 \longrightarrow NaCl + Cl$	0	11.6	11.58	1.0
$K + Br_2 \longrightarrow KBr + Br$	0	12.0	11.47	3.4
$K + HBr \longrightarrow KBr + H$	0.2	11.6	11.46	1.3
$Br + H_2 \longrightarrow HBr + H$	19.7	11.43	11.60	0.7
$Cl + H_2 \longrightarrow HCl + H$	4.3	10.92	11.59	0.22
$F + H_2 \longrightarrow HF + H$	1.13	11.06	11.55	0.32
$O + H_2 \longrightarrow OH + H$	11.3	10.4	11.53	0.07
$D + H_2 \longrightarrow HD + H$	7.61	10.64	11.60	0.11
$O + ClO \longrightarrow O_2 + Cl$	0.1	10.35	11.06	0.19
$Cl + O_3 \longrightarrow ClO + O_2$	0.5	10.21	11.22	0.10
$O + O_3 \longrightarrow O_2 + O_2$	4.09	9.68	11.27	0.026
$O + NO_2 \longrightarrow O_2 + NO$	0.24	9.59	11.24	0.022
$O + CO_2 \longrightarrow O_2 + CO$	54.2	10.28	11.28	0.10
$OH + H_2 \longrightarrow H_2O + H$	4.17	9.67	11.63	0.011
$OH + CO \longrightarrow CO_2 + H$	1.08	8.62	11.33	0.0019
$CO + O_2 \longrightarrow CO_2 + O$	51.0	9.54	11.34	0.004
$NO + O_3 \longrightarrow NO_2 + O_2$	2.72	9.04	11.35	0.005
$CO + NO_2 \longrightarrow CO_2 + NO$	27.8	8.75	11.35	0.0025
$C_2H_4 + H_2 \longrightarrow C_2H_6$	43.0	6.09	11.81	0.0000019

[a] Activation energy E_a in kcal/mol and A in L mol^{-1} s^{-1}. A_{ct} prediction of collision theory (Equation 15.42 at $T = 298$ K) using molecular diameters d derived from viscosity measurements. Rate constants at a given T may be generated from $\log_{10}k = 1000E_a/(2.303RT) + \log_{10}A$, generally reproducing actual experimental values within 20%.

Because collision theory assumes that every reaction must occur *via* a collision, then the experimental results indicate that even if a collision occurs with sufficient energy to overcome the activation energy barrier, it may not result in reaction. This failure to react can be attributed to an orientation or *steric* effect, in which molecules may collide with sufficient energy, but with an "ineffective" orientation:

(a)

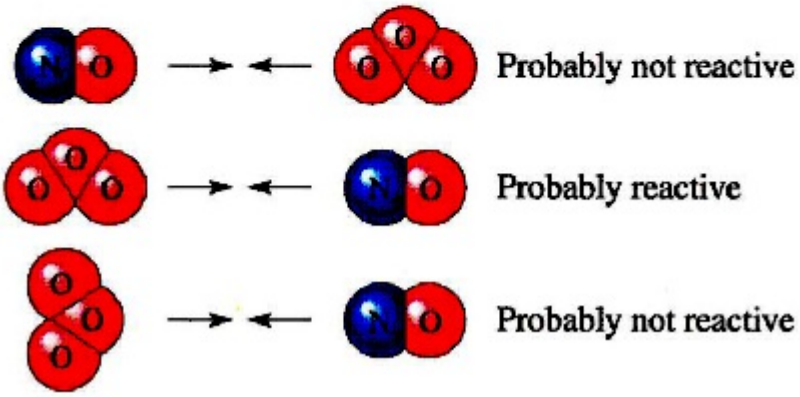

$2\ BrNO \longrightarrow Br_2 + 2\ NO$

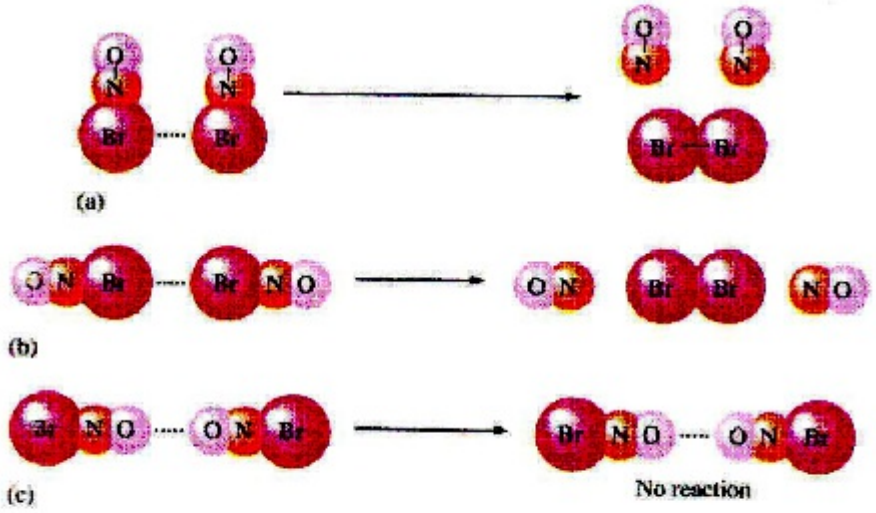

Figure 15.11
Several possible orientations for a collision between two BrNO molecules. Orientations (a) and (b) can lead to a reaction, but orientation (c) cannot.

$$2\,NOCl \longrightarrow Cl_2 + 2\,NO$$

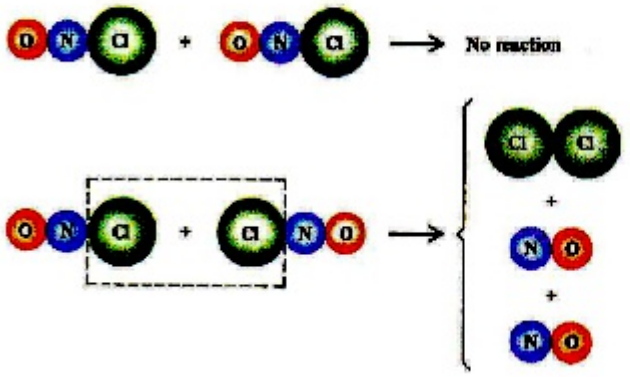

Figure 11-12
The steric effect on the probability of a reaction. The two NOCl molecules must approach each other in such a way that the two chlorine atoms are close together, if the encounter is to produce $Cl_2(g)$ and $NO(g)$.

Because collision theory gives equal weight to all collisions, including ones that are ineffective, it thereby overestimates the attempt rate, resulting in $p < 1$ and $p \ll 1$ in many cases. Additionally, the steric p factor is not easily calculated, which results in collision theory being a descriptive and conceptual model of chemical kinetic theory, rather than a predictive one.

The Lindemann Mechanism. Because collision theory is an inherently bimolecular model involving a second-order rate law, it seemingly omits many reactions that are known to be first-order. Reactions such as isomerizations and decompositions, which involve only a single reactant molecule, had been assumed to be first-order. However, in the 1920s Frederick Lindemann (and further developed by Cyril Hinshelwood) proposed that even these types of reactions are mediated by collisions.

Lindemann suggested that a generic first-order reaction, such as A → P, actually involves an initial *collisional activation* step in which two molecules of A collide with sufficient energy to cause one of them to become internally (*i.e.,* vibrationally) excited:

$$\begin{aligned} A + A &\underset{k_{-1}}{\overset{k_1}{\rightleftharpoons}} A^* + A \\ A^* &\xrightarrow{k_2} P \end{aligned} \qquad (14)$$

The excited A^* molecule then reacts to form P in a unimolecular process.

A rate law for the Lindemann-Hinshelwood mechanism can be developed by using the steady-state approximation for the concentration of the intermediate A^*:

$$\frac{d[A^*]}{dt} = k_1[A]^2 - k_{-1}[A^*][A] - k_2[A^*] = 0 \qquad (15)$$

Solving for $[A^*]$,

$$[A^*] = \frac{k_1[A]^2}{k_{-1}[A] + k_2} \qquad (16)$$

Hence, using the expression for $[A^*]$ from Eq. (16), the rate of formation of the product P is given by

$$\frac{d[P]}{dt} = k_2[A^*] = \frac{k_1 k_2[A]^2}{k_{-1}[A] + k_2} \qquad (17)$$

Two limiting cases for Eq. (17) can be defined. If the rate of deactivation of $[A^*]$ back to [A] greatly exceeds its rate of decomposition to P (*i.e.*, if $k_{-1}[A] >> k_2$), then

$$\frac{d[P]}{dT} = \frac{k_1 k_2}{k_{-1}}[A] = k_\infty[A] \qquad (18)$$

and the reaction appears to be unimolecular and first-order, even though bimolecular collisions are necessary for reaction to occur. This is the situation that is typically observed for most reactions when pressures are a few Torr or greater. (k_∞ represents the limiting value of the first-order rate constant at infinite pressure.)

On the other hand, if the pressure is sufficiently low, then the initial collisional activation is the rate-limiting step, *i.e.*, $k_2 >> k_{-1}[A]$, and the reaction appears to be second-order:

$$\frac{d[P]}{dT} = k_1[A]^2 \qquad (19)$$

These two limiting cases can be combined by defining an "apparent" first-order rate constant:

$$k = \frac{k_1 k_2}{k_{-1} + k_2[A]} \qquad (20)$$

which becomes pressure-dependent at low pressures (low [A]). Thus, the relative rate of reaction, (dP/dt)[A], is predicted to decrease at low [A]. This decrease in the effective first-order rate constant at low pressures is an important test of the Lindemann mechanism. The Figure below shows data for the "unimolecular" decomposition of cyclopropane to propylene over a wide range of pressures and illustrates the decrease of k at low pressures.

Figure 15.10
Dependence of the apparent first-order rate constant k on pressure for the isomerization of cyclopropane. At low pressure the slope of the plot of log k/k_∞ versus log pressure approaches unity, reflecting second-order kinetics, while at high pressure it goes to zero, and the reaction becomes first-order. *Source:* Pritchard et al., Proc. Roy. Soc. (1953).

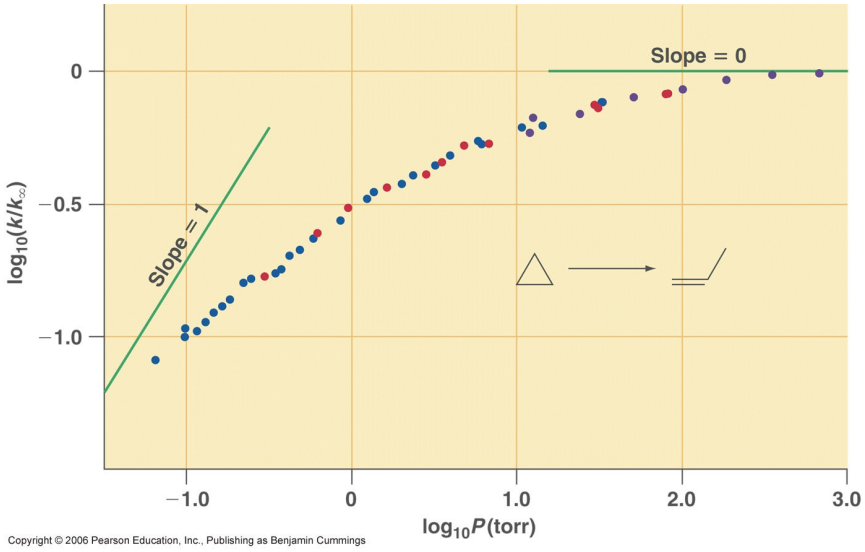

Transition State Theory

Originally developed by Henry Eyring in 1935 as a model for bimolecular reactions, Transition State Theory postulates that the transitory species which is formed as a reacting system passes over the activation barrier is a separate thermodynamic state, called the **activated complex** or the **transition state**. For the bimolecular reaction A + B → P, for example, the transition state is denoted by $AB^{\ddagger}$. Because this state lies atop the crest of the activation barrier, it is in *metastable equilibrium*, and a "mechanism" for its involvement in a bimolecular reaction is:

$$A + B \underset{k_{-1}}{\overset{k_1}{\rightleftharpoons}} AB^{\dagger} \xrightarrow{k_c} P \qquad (21)$$

If it is assumed that $AB^{\ddagger}$ is in equilibrium with A and B, *i.e.*, that decomposition of $AB^{\ddagger}$ is rate-limiting, then

$$K^{\dagger} = \frac{[AB^{\dagger}]}{[A][B]} \qquad (22)$$

where $K^{\ddagger}$ is the equilibrium constant for complex formation.

The rate of product formation is the rate at which $AB^{\ddagger}$ decays into products, which is an inherently unimolecular process:

$$\frac{d[P]}{dT} = k_c[AB^{\dagger}] = k_c K^{\dagger}[A][B] \qquad (23)$$

The basis of Eyring's theory is that the activated complex decomposes into products when a critical bond in $AB^{\ddagger}$ breaks. The force constant of the dissolving bond approaches zero, and its energy quantization is

therefore relaxed and can assume the classical energy $\varepsilon = k_B T$. According to Planck's hypothesis, the frequency corresponding to this energy is $\nu = \varepsilon / h = k_B T$. In the classical limit, this frequency becomes the classical frequency of motion along the direction of the dissolving bond. Thus, ν can be identified as the unimolecular rate constant k_c, and the bimolecular rate constant k for the overall reaction A + B → P is then

$$k = \frac{k_B T}{h} K^{\dagger} \tag{24}$$

According to classical thermodynamics, $K^{\ddagger}$ is also related to the Gibbs energy change for a reaction and, hence to the enthalpy and entropy changes by

$$-RT \ln K^{\ddagger} = \Delta G^{\circ\ddagger} = \Delta H^{\circ\ddagger} - T\Delta S^{\circ\ddagger} \tag{25}$$

where $K^{\ddagger}$ has inverse concentration units, *e.g.*, L/mol. Thus, Eq. (24) can be written

$$k = \frac{k_B T}{h} e^{\Delta S^{\circ\dagger}/R} e^{-\Delta H^{\circ\dagger}/RT} \tag{26}$$

Comparing Eq. (26) to Eq. (1), the Arrhenius activation energy, E_a, defined as the slope of a ln$k$ *vs.* $1/T$ plot, can be identified as

$$E_a = \Delta E^{\circ\ddagger} = \Delta H^{\circ\ddagger} - (\Delta n^{\ddagger} - 1)RT \tag{27}$$

where $\Delta n^{\ddagger}$ is the change in number of moles of gas in going from reactants to the transition state. For a bimolecular reaction, such as A + B → AB‡, $\Delta n^{\ddagger} = -1$, while for unimolecular reactions, $\Delta n^{\ddagger} = 0$, as it is for all condensed-phase reactions. At normal temperatures, the difference between $\Delta E^{\circ\ddagger}$ and $\Delta H^{\circ\ddagger}$ is only a few kJ/mol. Thus, the Arrhenius frequency factor can be identified from Eq. (26) as

$$A = \frac{k_B T}{h} e^{\Delta S^{\circ\dagger}/R} e^{(1-\Delta n^{\dagger})} \tag{28}$$

The collision theory model results in a single unknown quantity that must be experimentally measured, *viz.*, the Arrhenius activation energy, E_a. Transition state theory, by contrast, results in two unknown quantities, E_a (or $\Delta H^{\circ\ddagger}$) and $\Delta S^{\circ\ddagger}$. However, because the transition state model is based on thermodynamics, it is possible to use statistical thermodynamic methods to predict at least reasonable estimated values for $\Delta S^{\circ\ddagger}$. Despite the approximations involved in postulating vibrational frequencies for the $AB^{\ddagger}$ complexes, and, hence, their partition functions, predictions by the transition state model are far superior to those of collision theory.

Molecular Reaction Dynamics

Real molecular collisions in the gas phase are more complex than the simple "billiard ball" model would suggest. Molecular attractions (van der Waals forces) and repulsions (Pauli exclusion principle) play important roles in governing trajectories of molecular encounters:

Figure 15.11

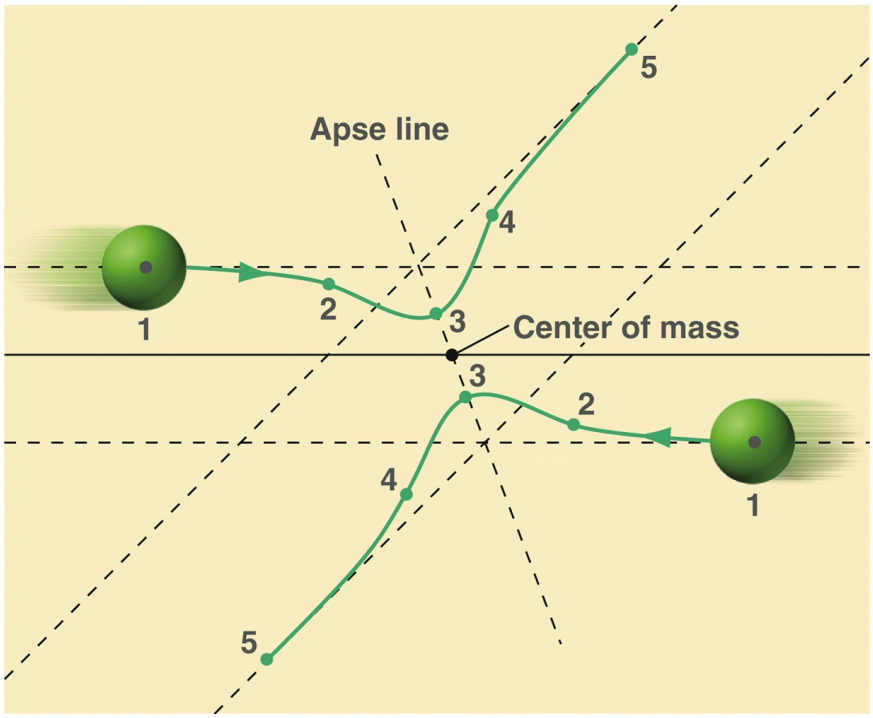

Collision trajectories for two atoms under the influence of van der Waals forces. The numbers indicate the passage of time; the total duration of the collision, from $t = 1$ to $t = 5$, is of the order of a picosecond or less. With the center of mass of the atoms held stationary, the atoms approach each other and recede after collision along straight lines (Newton's first law) from opposite directions. For identical atoms, the trajectories exactly mirror each other, the force on one atom always accompanied by an equal and opposite force on the other (Newton's third law). The shapes of the trajectories are determined by Newton's second law. When the atoms are still rather far apart ($t = 2$), the attractive London dispersion (LD) force begins to accelerate them toward each other. The overlap (Pauli) repulsive force then takes over until the two atoms "touch" at $t = 3$, and they recede with gracefully symmetric motion through the attractive region ($t = 4$) before resuming undisturbed linear paths. Each trajectory is symmetric about the "apse line." Molecular trajectories are more complex due to orientational effects and rotation/vibration within each molecule, but are roughly of the same form.

Atom-molecule reactions of the type A + BC → AB + C are often elementary steps in the mechanisms of gas-phase reactions involving simple diatomic molecules. In this type of reaction, one bond is broken, and one is made, and the molecular mechanics can be modeled as occurring in three steps:

1. A · · · · · · B — C
2. A · · · B · · · C
3. A — B · · · · · · C

A approaches BC; the new A-B bond begins to form, while the original B-C bond begins to break, and finally the liberated C atom departs from the newly formed AB molecule. The energetics of reactions such as this are conveniently displayed on three-dimensional *potential energy surfaces*, which depict the changes in both bond lengths on the two horizontal axes and the potential energy on the vertical axis:

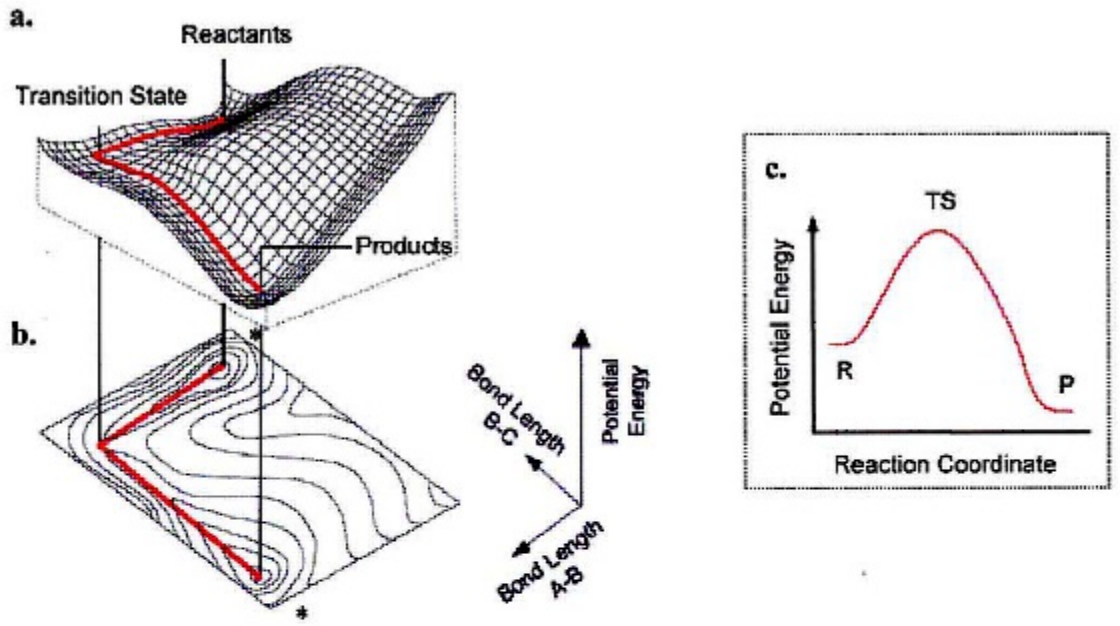

Figure 1.3. (a.) Cartoon of the three-dimensional potential energy surface for the reaction A-B + C → A + B-C. The reactants and products are found in potential energy wells and the reaction pathway (red line) follows a minimum energy route. The transition state occupies a saddle point on the reaction pathway which means that the activated complex has only two paths in which it can obtain lower potential energy, by returning to the reactant formation or continuing on to form products. (b.) The same potential energy surface projected into two dimensions for easier interpretation. The topographical lines represent regions of degenerate energy and the asterisks (*) mark the equilibrium bond length for A-B and B-C. (c.) The reaction coordinate diagram distills the reaction information from figures like A and B, which contain unique variables for characterizing a particular reaction, to a set of uniform variables, potential energy and reaction coordinate. The diagram comes from the cross section of (a.) and (b.) through the red line and reflects potential energy changes as the reaction progresses. (R = reactants, TS = transition state, P = products)

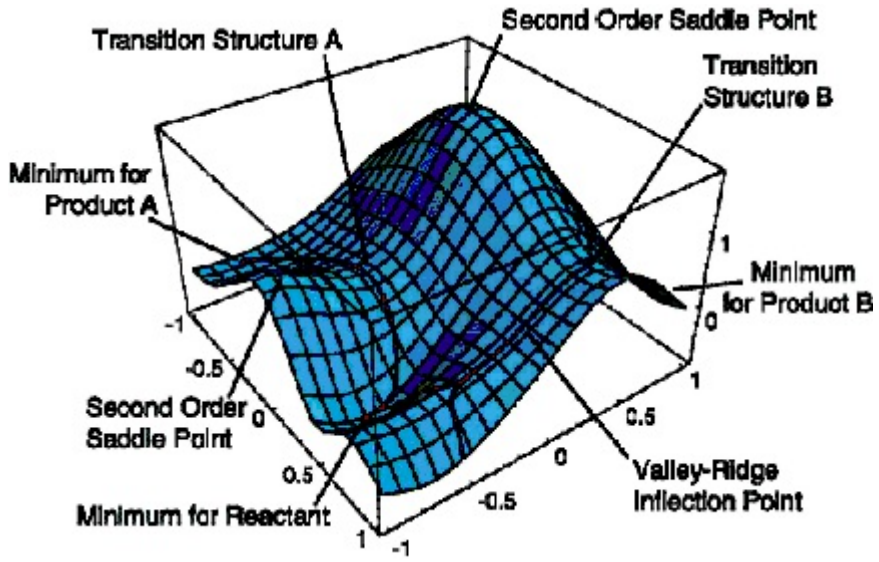

Examples of such an elementary reaction are

$$F + H_2 \rightarrow HF + H$$

and

$$H + F_2 \rightarrow HF + F$$

which are steps in the mechanism of the bimolecular reaction

$$H_2 + F_2 \rightarrow 2\ HF$$

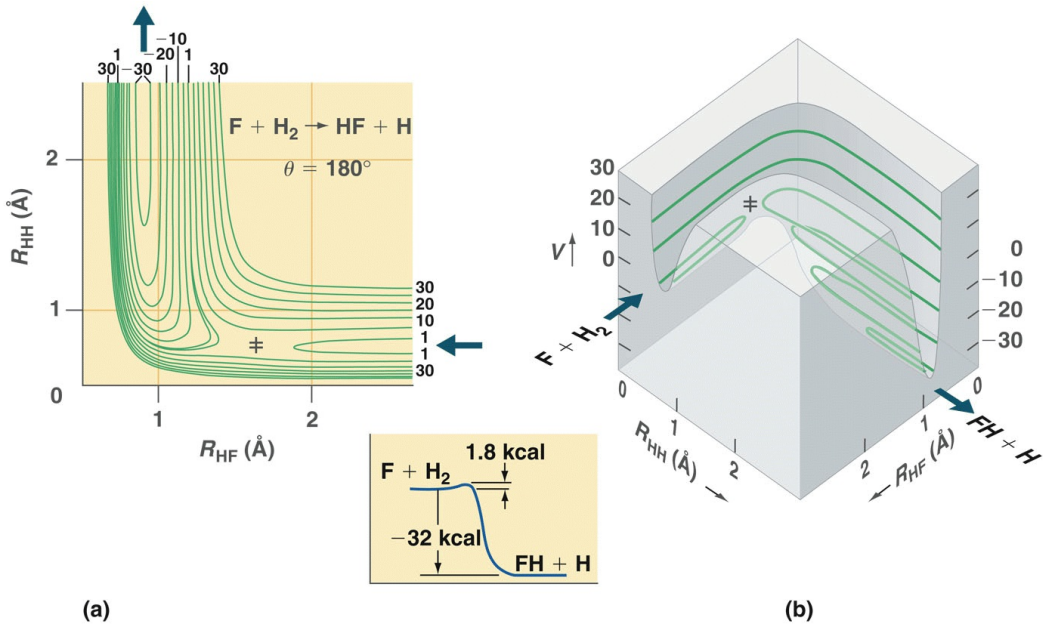

Figure 15.12
Depictions of the potential energy surface for the reaction $F + H_2 \longrightarrow HF + H$ based on a recent highly accurate molecular orbital calculation (Stark & Werner, *J. Chem. Phys.*, 1996). **(a)** Potential energy contour map for collinear $F \cdots H \cdots H$ geometry ($\theta = 180°$ is the bond angle). Contours are drawn every 5 kcal/mol for +30 to −30 kcal, with one extra contour added for $V = 1$ kcal in order to delineate the activation barrier, whose location is indicated by ‡. Reagents enter from the lower right, where R_{HF} is large and R_{HH} is at equilibrium for H_2 at the lowest point, and products emerge at the upper left, where R_{HH} is large and R_{HF} is now at equilibrium. The difference in energy between these extremes is 31.8 kcal/mol, which is the exothermicity of the reaction; the barrier height is 1.8 kcal, in good agreement with E_a from Table 15.4. **(b)** This surface is shown as a groove cut into a transparent block; for clarity, only half of the contours are drawn, with the positive-energy ones on the large-R edge of the groove omitted. It is more easily seen here than in (a) that the extremes represent bond potential energy curves for the two diatomics. The inset shows the corresponding energy profile.

Figure 15.12

Depictions of the potential energy surface for the reaction $F + H_2 \longrightarrow HF + H$ based on a recent highly accurate molecular orbital calculation (Stark & Werner, *J. Chem. Phys.*, 1996). **(a)** Potential energy contour map for collinear $F \cdots H \cdots H$ geometry ($\theta = 180°$ is the bond angle). Contours are drawn every 5 kcal/mol for +30 to −30 kcal, with one extra contour added for $V = 1$ kcal in order to delineate the activation barrier, whose location is indicated by ‡. Reagents enter from the lower right, where R_{HF} is large and R_{HH} is at equilibrium for H_2 at the lowest point, and products emerge at the upper left, where R_{HH} is large and R_{HF} is now at equilibrium. The difference in energy between these extremes is 31.8 kcal/mol, which is the exothermicity of the reaction; the barrier height is 1.8 kcal, in good agreement with E_a from Table 15.4. **(b)** This surface is shown as a groove cut into a transparent block; for clarity, only half of the contours are drawn, with the positive-energy ones on the large-R edge of the groove omitted. It is more easily seen here than in (a) that the extremes represent bond potential energy curves for the two diatomics. The inset shows the corresponding energy profile.

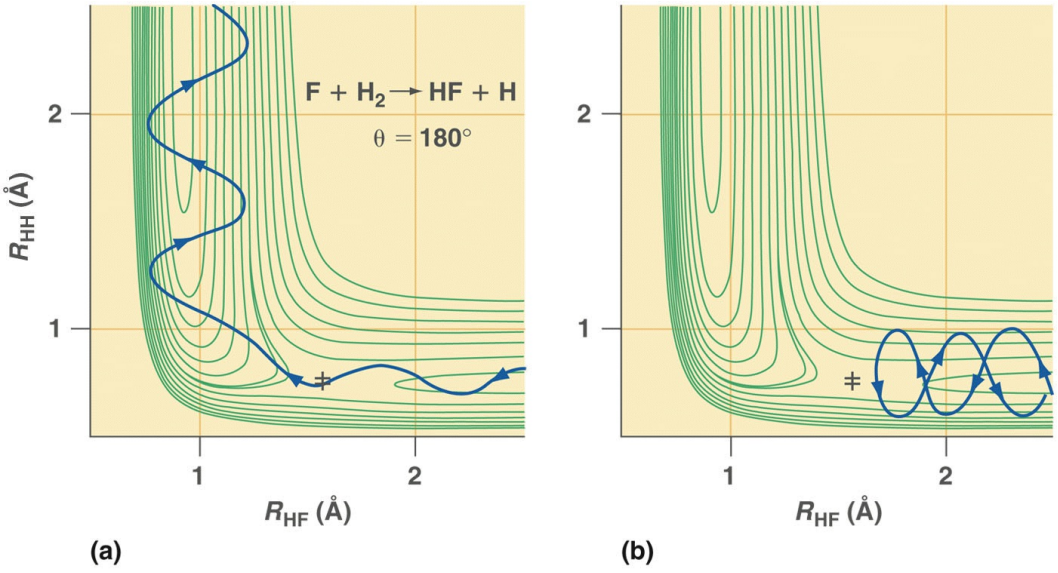

A similar reaction to the above is $H_2 + Br \rightarrow H + HBr$, for which the potential energy surface is shown below. Note that the energetics (E_a = 84 kJ and ΔE_r° = +63 kJ) for this closely-related reaction are quite different from the corresponding values for the $F + H_2$ reaction above, for which E_a = 7.5 kJ, and ΔE_r° = −134 kJ.

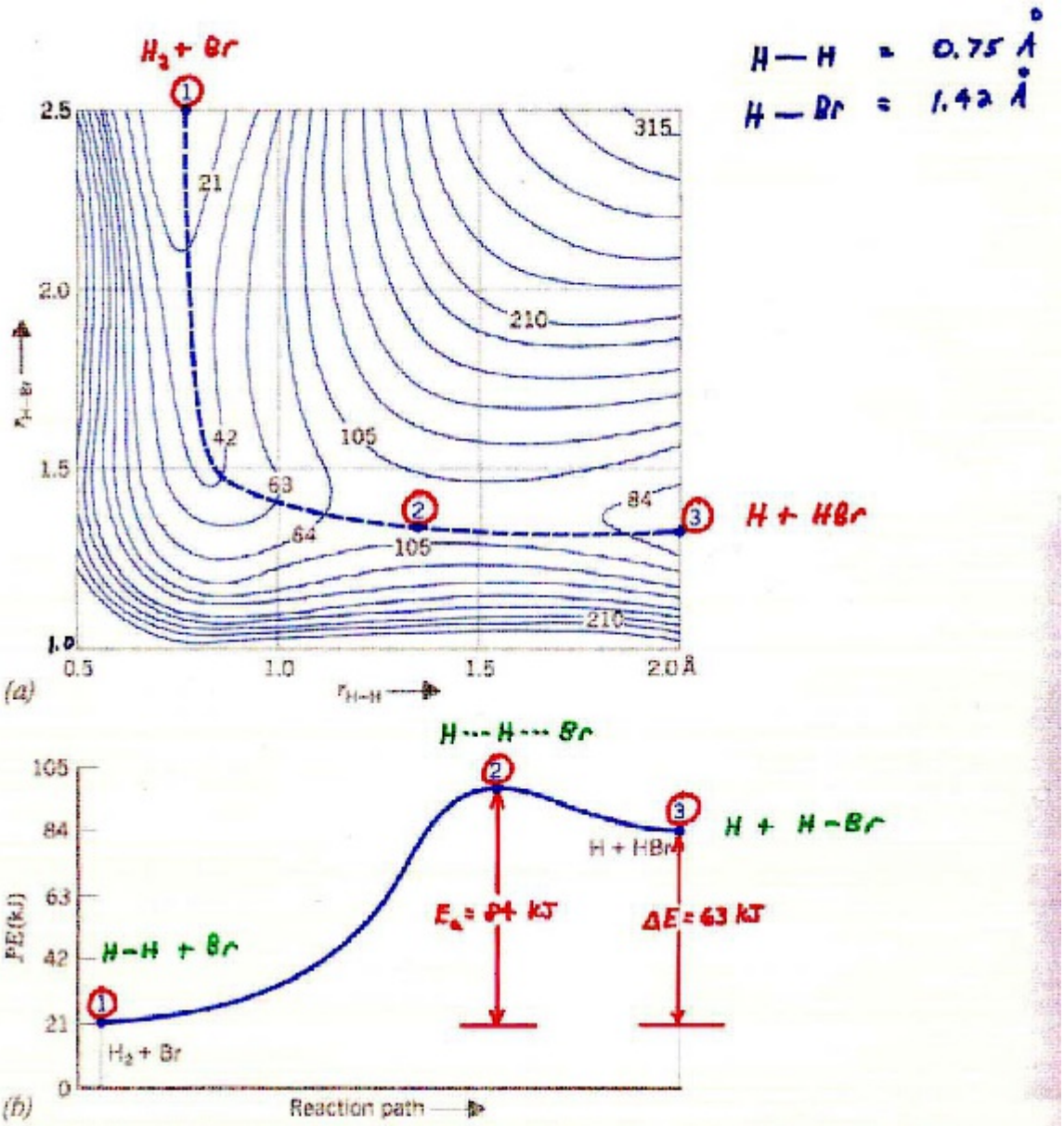

Fig. 19.14. *(a)* Contour diagram of the potential energy surface for the reaction $H_2 + Br \rightarrow H + HBr$ as a function of the internuclear distances r_{H-Br} and r_{H-H} in angstroms. All three atoms are assumed to be collinear throughout the reaction. Contours of equal potential energy are marked in kilojoules per mole. Point 1 is the initial state, with a Br atom far from an H_2 molecule. Point 3 is the final state, with an H atom far from an HBr molecule. The reaction pathway is indicated by the dashed colored line, which is the path that requires crossing the lowest possible potential energy contours between points 1 and 3. Point 2 is the activated complex, the state of highest potential energy along the reaction pathway. *(b)* A potential energy profile of the reaction pathway. Points 1–3 represent the same states as points 1–3 on the contour diagram. Note that this is an endothermic reaction, as the products are at a higher energy than the reactants.